Y/DW-983
Proceedings

Y-12

OAK RIDGE
Y-12
PLANT

MARTIN MARIETTA

FAST, HIGH RESOLUTION X-RAY MICROFLUORESCENCE IMAGING

D. A. Carpenter, M. A. Taylor
Development Division

August 15, 1990

For Submission to the
39th Annual Denver X-ray Conference
Steamboat Springs, CO
July 29 - August 3, 1990

Prepared by the
Oak Ridge Y-12 Plant
P.O. Box 2009
Oak Ridge, Tennessee 37831
operated by
MARTIN MARIETTA ENERGY SYSTEMS, INC.
for the
U.S. DEPARTMENT OF ENERGY
under contract DE-AC05-84OR21400

MANAGED BY
MARTIN MARIETTA ENERGY SYSTEMS, INC.
FOR THE UNITED STATES
DEPARTMENT OF ENERGY

Y/DW--983

DE91 010658

Fast, High-Resolution X-Ray Microfluorescence Imaging

D. A. Carpenter and M. A. Taylor

Martin Marietta Energy Systems, Inc.
Oak Ridge Y-12 Plant[a]
Oak Ridge, Tennessee 37831-8084

INTRODUCTION

X-ray microfluorescence imaging refers to the use of an x-ray beam as a probe to excite XRF in a specimen and produce a spatially resolved image of the element distribution. The advantages of high sensitivity and low background, together with the nondestructive nature of the measurement, have lead to applications of x-ray microfluorescence analysis in biology, geology, materials science, as well as in the area of nondestructive evaluation. Previous reports have described the development of an x-ray microprobe which uses a conventional source of x-rays to produce a 10-μm beam.[1,2,3] This paper describes improvements to the microprobe which have increased the beam power and the solid angle of detection. The data collection and display software have also been enhanced.

DESCRIPTION OF SYSTEM IMPROVEMENTS

The basic approach to high beam brilliance with a conventional source was to use a glass capillary tube positioned near the focal spot of a high-brilliance microfocus x-ray tube.[1] Previous studies had shown that the maximum allowable power density with a microfocal spot can be several orders of magnitude greater than that allowable with a typical x-ray tube having a macrofocal spot.[4] In addition, the glass capillary tube was a guide tube for the x-rays, producing an intense beam with a uniform profile.

The x-ray tube used for the microprobe source was the IRT-Ridge (San Diego, CA) model HOMX-160A, designed primarily for real-time x-ray radiography applications. The HOMX-160A has unique features which allow close-coupling with the glass capillary. These features include (1) an externally adjustable beam deflection coil to align the focal spot with the stationary glass capillary tube, (2) a vacuum pumping system permitting access to the inside of the tube, and (3) a replaceable anode head.

[a]This work was performed at the Oak Ridge Y-12 Plant, which is operated by Martin Marietta Energy Systems for the US Department of Energy under Contract number DE-AC05-84OR21400.

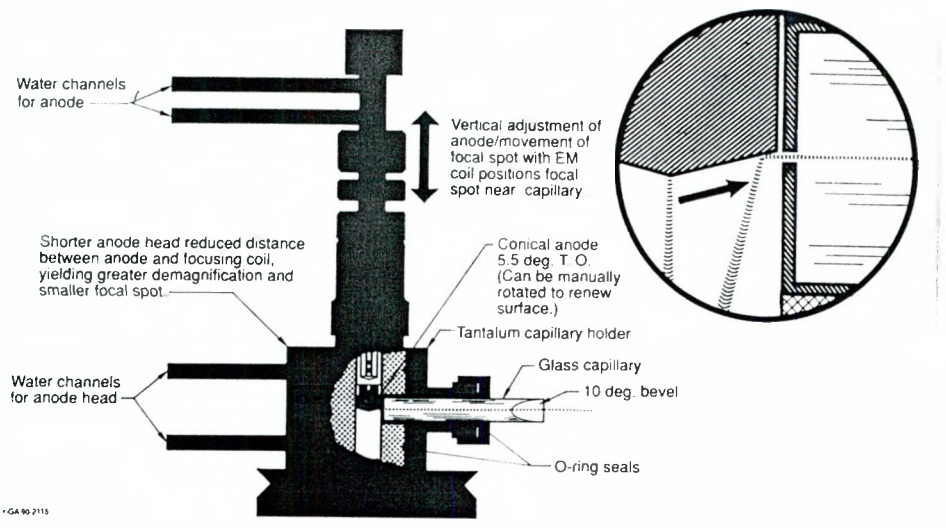

Figure 1 Modifications made to the short anode head to increase the beam flux of the x-ray microprobe.

Initially, a holder for the glass capillary tube replaced the x-ray tube window. The holder positioned one end of the capillary about 5 mm from the center of the anode. With a 10-μm capillary, that arrangement provided a 180-fold intensity gain over a comparable pinhole aperture.[1] However, the system still lacked adequate intensity for rapid microfluorescence scans.

The system was modified by redesigning the anode head to (1) reduce the distance between the focusing magnet and the anode and, thus, reduce the size of the focal spot, (2) decrease the distance between the focal spot and the capillary tube and increase the solid angle of radiation intercepted by the capillary, and (3) provide water-cooling for the anode head body and the anode. The schematic of the new anode head in Fig. 1 illustrates those changes.

The distance between the focusing magnet and the target anode was reduced by a factor of 0.5 by exchanging the long anode head, originally supplied by IRT-Ridge, with their short anode head. The demagnification of the electron beam is given by the ratio r_2/r_1, where r_1 is the distance between the filament and the end of the focusing magnet and r_2 is the distance between the end of the focusing magnet and the target anode. The reduction of the focusing distance decreased the focal spot diameter from 30 μm at 30 kV and 9 watts to about 15 μm.[b] The latter diameter was consistent with the estimate given by Grider, et.al.[4]

The short anode head was then modified in the following ways. First, the anode was attached to a threaded shaft which could be positioned vertically by ± 3 mm about the

---

[b]Grider, et. al. (Ref. 5) pointed out that the load on the target anode is actually less than that measured by the HOMX 160. Beam current is measured in the area of the cathode, whereas the actual current reaching the target anode, at ground potential, might be significantly less than the current in the cathode region. According to their measurements on a modified tube head, the maximum load on the target anode before the onset of melting, ranges from 6 to 11 watts, depending upon the target anode material. Therefore, in the x-ray microprobe work, we assume that molybdenum targets are loaded at about 6 watts and tungsten targets are loaded at about 9 watts.

Table 1

Beam Parameters of the Oak Ridge Microprobe

Capillary Size	Anode	Ni kα Fluorescence (c/s)	Beam Power (c/s)
10 μm	Mo	3300	8×10^5
10 μm	W	6865	7×10^5

Capillaries were pyrex glass; 100 mm long for Mo, 59 mm long for W.

centerline of the capillary. The new anode, now conical instead of flat, had a cone angle of 89 deg. and presented a 5.5 deg. takeoff angle to the capillary. As illustrated by the inset of Fig. 1, it was possible to find a vertical anode position where the focal spot was near the edge of the anode when it was aligned with the capillary channel. The vertical adjustment of the anode reduced the minimum focal spot-to-capillary distance from 5 mm to about 2 mm. For an ideal point source, a 6-fold intensity gain was calculated due to the increase in the solid angle of radiation striking the anode end of the capillary. Because of the finite size of the focal spot, the actual measured gains for the tungsten and molybdenum anodes were 2- to 3-fold.

The new design also permitted rotation of the conical anode to renew the focal surface. Finally, as shown in Fig. 1, cooling water channels were added to the body of the anode head and to the anode shaft for thermal stability.

To increase the solid angle of detection, the Si(Li) detector (30 mm^2) was replaced by a new Si(Li) detector with a larger crystal (50 mm^2), located nearer the end of the cryostat. The new detector provided a 3.7-fold increase in the detected fluorescence intensity with some loss of resolution (170 ev as opposed to 150 ev for the old detector).

Table 1 shows the results of the system improvements. The beam power data were determined from the Ni fluorescence intensity, the geometry of the system (beam-specimen angle = 90 deg., specimen-detector angle = 45 deg.), and the detector solid angle ($d\Omega/4\pi = 2.86 \times 10^{-2}$). The energy of the Mo kα line was assumed to be the effective wavelength in the case of the Mo anode. For the tungsten anode, the L lines of tungsten were

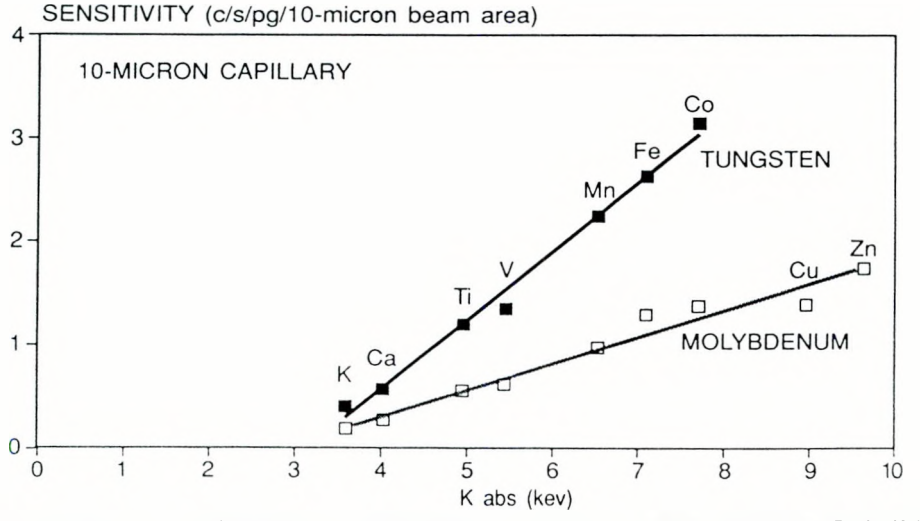

Figure 2 Sensitivity as a function of elemental absorption edges for the Oak Ridge microprobe from NIST thin film standards, SRM 1832 and 1833.

assumed to compose the effective wavelength. The tungsten L lines were weighted according to the published spectral distribution.[5] Typical element sensitivities were determined from NIST standards 1832 and 1833 by scanning over large areas in a 45-45 deg. geometry. Fig. 2 shows the sensitivity results.

DATA COLLECTION AND DISPLAY ENHANCEMENTS

Two data collection systems were developed to provide up to 57,000 pixels of imaging data in a 300 x 190 pixel^2 format. Counting times typically range from 0.01 to 5 s/pixel. Both systems scan "on-the-fly". The x,y positioner sends out pulses to the stepper motors of the sample stage at a rate corresponding to the desired x-ray counting time. Simultaneously, pulses from the positioner are sent to a counter/timer. At a preset number of pulses corresponding to the x-ray counting time, the counter/timer outputs a signal to the 80386 processor. In the HIGHCNT routine, the processor reads and resets a counter corresponding to each region-of-interest (ROI) that had been previously defined in a Tracor Northern TN-7200 multichannel analyzer. The MCA acquires spectral data continously during a run. A maximum of four ROI's may be defined for the HIGHCNT routine. In addition, HIGHCNT allows the accumulation of a maximum of 64,000 counts/pixel/ROI.

A second routine, FASTRUN, permits data from 10 ROI's to be collected. The ROI's for FASTRUN are selected from an internal MCA board. The 80386 processor reads, sums, and resets memory locations corresponding to the pre-selected ROI's, while the MCA acquires data continuously. A maximum of 256 counts/pixel/ROI is permitted. Although the maximum allowed number of counts is low for quantitative analysis, good qualitative element images can be created with only a few counts/pixel because of the high peak-to-background ratio produced by excitation with x-rays.

Both data acquisition routines store the XRF data in computer memory during a horizontal line scan. At the end of each line scan and before the positioner increments the vertical axis, the line-scan data is transfered to RAMdisk memory. The amount of data lost during continuous scanning is small because of the low overhead of the data acquisition techniques.

Data processing typically consists of a histogram correction procedure followed by display with commercially available display programs. A VGA graphics card is used with a standard color monitor. Standard image enhancement techniques, accessible from a commercially available shareware routine called VGACAD[6], are used occasionally. Additional processing is available through a routine (COLOR) which combines three ROI's into one image by mixing colors. The data from each ROI is scaled to 16 or 32 grey scales of either red, green, or blue. The combined image is produced by overlaying the three ROI's on a pixel by pixel basis in VGA graphics. The red, green, and blue color intensities can be adjusted interactively to reveal detailed elemental spatial relationships.

APPLICATION EXAMPLES

Two examples illustrate the results of the data collection scheme and the utility of the color mixing routine. Molybdenum radiation was used to construct both images. Fig. 3 compares an SEM backscatter micrograph with a color-combined x-ray microfluorescence image of a malachite ore. The 300 x 190 pixel^2 microfluorescence image required 16 minutes of data collection time at 0.01 s/pixel and a pixel size of 10 x 10 μm^2. The SEM micrograph suffers from low contrast due to small differences in atomic numbers, in addition to charging around voids and cracks. The microfluorescence image complements the SEM

Figure 3 Comparison of SEM backscatter micrograph of a malachite ore (left) with a color-combined x-ray microfluorescence image (right).

Figure 4 X-ray microfluorescence images of tungsten (top, left), nickel (top, right), iron (bottom, left) and the color-combined image (bottom, right).

analysis by providing enhanced contrast.

Fig. 4 shows microfluorescence images of the elements composing a tungsten-5wt% nickel-2.5wt% iron (W-Ni-Fe) alloy. The pixel sizes in Fig. 4 are 2 x 2 μm^2 with 0.05 s/pixel counting time. The W-Ni-Fe alloy is a liquid-phase sintered alloy consisting of almost pure tungsten grains surrounded by a BCC phase of nickel, iron, and a small amount of tungsten. X-ray microfluorescence imaging affords a nondestructive method of examining parts made from the W-Ni-Fe alloy. With the 10-μm capillary, the system can resolve the 5-μm grain boundary shown on the tungsten image. The color combined image on the lower right of Fig. 5 reveals voids which are caused by gases entrapped during sintering. The voids act as crack initiation sites and are deleterious to the physical properties of the alloy.

REFERENCES

(1) D. A. Carpenter, "Improved Laboratory X-Ray Source for Microfluorescence Analysis", X-Ray Spectrometry, 18:253 (1989).
(2) D. A. Carpenter, M. A. Taylor, C. E. Holcombe, "Applications of A Laboratory X-Ray Microprobe to Materials Analysis", in: Advances in X-Ray Analysis, 32:115, C. S. Barret, J. V. Gilfrich, R. Jenkins, T. C. Huang, P. K. Predecki, eds, Plenum Press, New York (1989).
(3) D. A. Carpenter, R. L. Lawson, M. A. Taylor, D. E. Poirier, K. Z. Morgan, and G. W. Haney, "A Scanning X-Ray Microprobe with Glass Capillary Collimation", in: Microbeam Analysis, D. E. Newbury, Ed., San Francisco Press, San Francisco, 391 (1988).
(4) D. E. Grider, A. Wright, P. K. Ausburn, "Electron Beam Melting in Microfocus X-Ray Tubes", J. Phys. D: Appl. Phys., 19:2281 (1986).
(5) R. Tertian and F. Claisse, "Principles of Quantitative X-Ray Fluorescence Analysis", Heyden, London, 1982.
(6) VGACAD available from Dr. Marvin Gozum, 2 Independence Place Apt. 303-2, 6th and Locus Street, Philadelphia, PA 19106.

An X-ray microprobe scan of malacite ore (right) was used to complement SEM analysis (left). Note the low contrast in the SEM image due to small differences in atomic numbers. In addition, charging occurred around voids and cracks, in spite of the use of a conductive coating. Only 16 minutes were required to collect the 57,000 pixels of X-ray microprobe data. The element fluorescence data were combined using a color mixing routine to enhance contrast and facilitate the analysis.

Beam size: 10 μm
Pixel size: 10 x 10 μm^2
Radiation: Mo-k_α

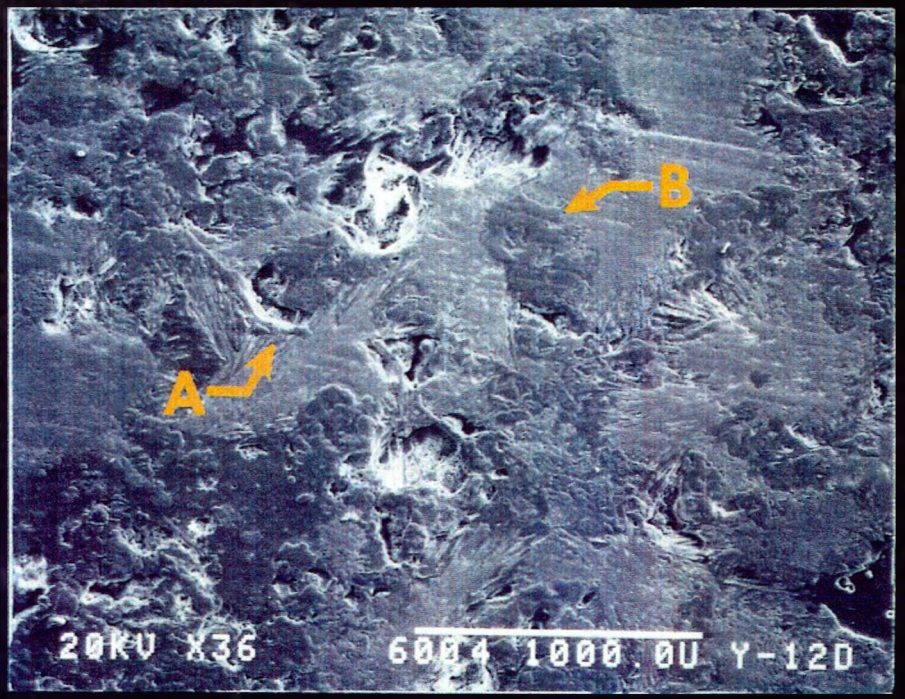

SEM Micrograph

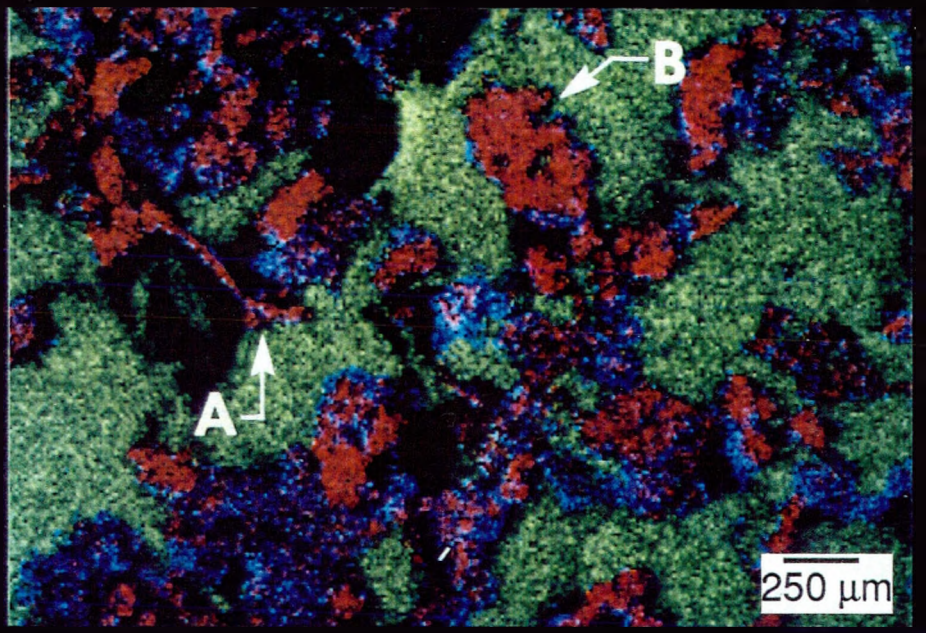

GREEN = Cu
RED = Fe
BLUE = Mn

Figure 3

Fig 3

The Tungsten-5wt% Nickel-2.5wt% Iron alloy is a liquid-phase sintered alloy consisting of almost pure tungsten grains surrounded by a BCC phase of Ni, Fe, and a small amount of W. Element images constructed from X-ray microprobe data show partially resolved grain boundaries down to approximately 5 µm. A color combination of the three element images reveals voids caused by gases entrapped during sintering. These voids are deleterious to the physical properties of the material.

Beam Size: 10 µm
Pixel size: 2 x 2 µm² (57,000 pixels)

Count time/pixel: 0.05 s
Radiation: Mo-k_α

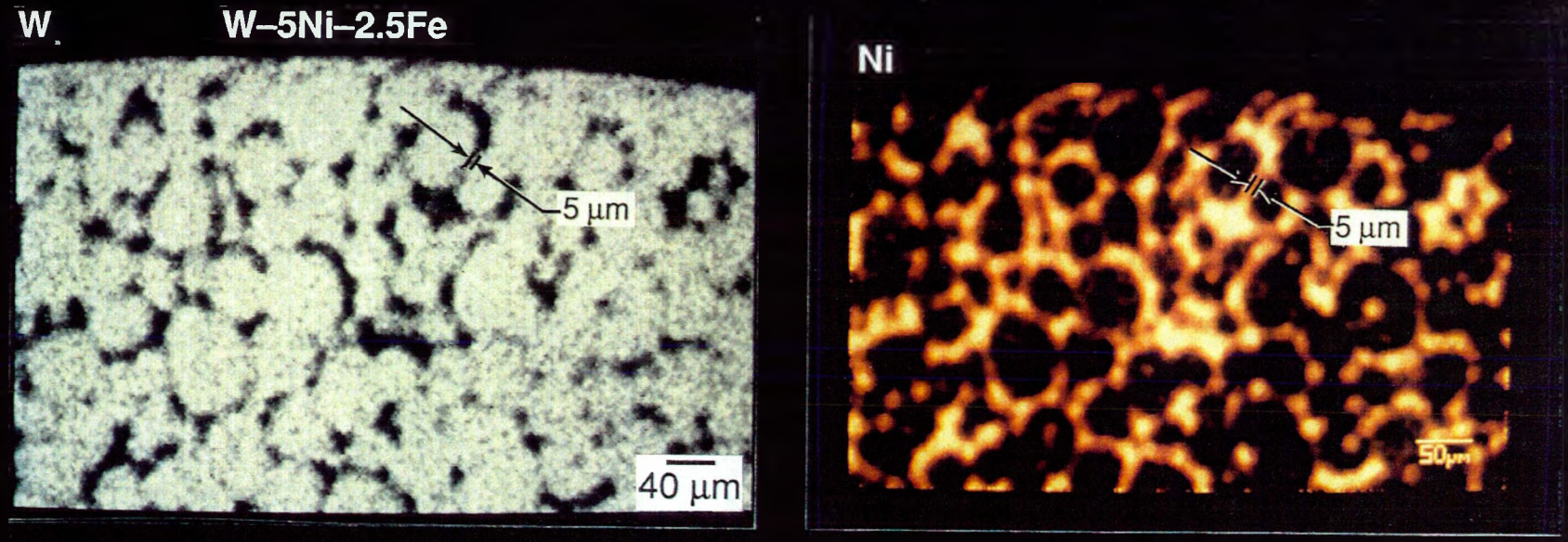

Figure 4

fig 4

Distribution:

D. A. Carpenter
D. H. Johnson/D. N. Braski
J. E. Keyes (2)
Y-12 Central Files